Post-coordination Backbone Functionalization of an Imidazol-2-Ylidene and Application to the Synthesis of Heteropolymetallic Complexes Incorporating the Ambidentate $IMes^{CO2-}$ Ligand

Dmitry A. Valyaev, Marina A. Uvarova, Alina A. Grineva, Vincent César, Sergei N. Nefedov, Noël Lugan

ELECTRONIC SUPPLEMENTARY INFORMATION

Table of contents

General information

All manipulations were carried out using Schlenk techniques under an atmosphere of dry nitrogen. Dry and oxygen-free organic solvents (THF, Et_2O, CH_2Cl_2, toluene) were obtained using LabSolv (Innovative Technology) solvent purification system. Acetonitrile was distilled over CaH_2 under argon atmosphere just prior to use. Solvents used for column chromatography (hexane, toluene, Et_2O, CH_2Cl_2) were deoxygenated by nitrogen bubbling during 15-20 min. Deuterated benzene for NMR experiments was deoxygenated by three freeze-pump-thaw cycles and kept over 4Å molecular sieves. Technical quality cymantrene purchased as anti-knocking fuel additive in TPL Region Company (Moscow, Russia) was purified by recrystallization from hexane at –20°C (*vide infra* for details). IMes.HCl,[1] (1,10-Phen)Cu(OAc)$_2$[2] and (1,10-Phen)Cu(OAc)$_2$[3] were prepared according to literature procedures. All other reagent grade chemicals purchased from commercial sources were used as received.

All photochemical procedures were performed in 250 mL reactor with an immersed 150 W Hg medium pressure lamp cooled by a quartz jacket with circulating water. Chromatographic purification of the compounds was performed on silica (0.060-0.200 mm, 60 Å) and activated alumina (neutral, 0.050-0.200 mm) obtained from Acros Organics and flushed with nitrogen just before use.

Solution IR spectra were recorded in 0.1 mm CaF_2 cells using a Perkin Elmer Frontier FT-IR spectrometer and given in cm^{-1} with relative intensity in parentheses. ^1H, ^{13}C and ^7Li NMR spectra were obtained on Bruker Avance 400 and Avance III HD 400 spectrometers and referenced to the residual signals of deuterated solvents[4] (^1H and ^{13}C) and 1M LiCl in D_2O (^7Li, internal standard), respectively. X-band ESR spectra for complex **4** were obtained using Bruker Elexys E500 spectrometer and simulated by EasySpin 5.0.18 software[5] in the anisotropic mode using Neider/Mead downhill simplex method (rsmd = 0.0841). Solution magnetic susceptibility for complex **4** was determined by Evans method in CD_2Cl_2 using Wilmad coaxial insert and then corrected for the diamagnetic ligands contribution.[6] Elemental analysis was carried out in LCC du CNRS (Toulouse, France) using Perkin Elmer 2400 series II analyzer.

Purification of technical quality cymantrene. Technical cymantrene (*ca.* 100 g) was charged on the top of column of silica (5×10 cm) and repeatedly extracted with 50 mL portions of warm hexane (40-50°C) until complete dissolution of the yellow product (10-15 extractions). The extracts were rapidly filtered through SiO_2 column to leave brown insoluble decomposition products at the top of the column. The combined extracts were kept in the freezer overnight at –20° C to give large yellow crystals. The solution was removed by decantation and the product was washed with hexane (150 mL) at –30°C to remove the traces of organic impurities (cyclopentadiene oligomers) and dried under vacuum to afford the first crop of pure cymantrene (50-60 g). The supernatant was concentrated to *ca.* 30% of its initial volume and cooled again at –20°C overnight. After removal of the solution by decantation, washing the product with hexane (2×50 mL) at –30°C and drying under vacuum the second crop of pure cymantrene (10-15 g) can be obtained.

Synthesis of (η^5-C_5H_5)$(CO)_2$Mn(IMes) (1). To a suspension of IMes.HCl (1.7 g, 5.00 mmol) in THF (50 mL) KHMDS (11 mL of 0.5 M solution in toluene, 5.50 mmol) was added dropwise under stirring at room temperature. After sonication of the reaction mixture (10 min) and subsequent stirring for additional 10 min the resulting yellow solution was evaporated and dried under vacuum. The residue was dissolved in toluene (220 mL) and transferred by cannula into the photochemical reactor charged with a stirring bar and cymantrene (1.02 g, 5.00 mmol). The resulting yellow solution was irradiated with UV light under vigorous stirring at room temperature until the ν_{CO} bands 1915 and 1847 cm^{-1} corresponding to the NHC complex **1** in IR spectrum of reaction mixture ceased to increase (*ca.* 2 h). The solution was filtered through a short alumina column (2×8 cm) using toluene as an eluent, the resulting yellow solution was concentrated to *ca.* 50 mL volume and hexane (100 mL) was slowly added under stirring to induce the crystallization of complex **1** finished at –20°C overnight. The supernatant was decanted and yellow precipitate was washed with hexane (20 mL) and dried to give the major crop of complex **1** as yellow crystals (1.6 g). The remaining solution was evaporated under vacuum and the resulting yellow residue was purified on a silica column (2×8 cm). Starting cymantrene was eluted as a light yellow band with hexane followed by a yellow-orange band of **1** eluted with toluene. Evaporation of the solvent under vacuum afforded a second crop of a complex **1** (0.42 g) for 84% total yield. Analytical data were consistent with a previous report.[7]

1: ^{1}H NMR (400.1 MHz, C_6D_6, 25°C): δ 6.86 (s, 4H, C*H*$_{Mes}$), 6.18 (s, 2H, C*H*$_{Im\text{-}4,5}$), 4.01 (s, 5H, Cp), 2.16 (s, 6H, C*H*$_{3para\text{-}Mes}$), 2.07 (s, 12H, C*H*$_{3ortho\text{-}Mes}$); ^{1}H NMR (400.1 MHz, $(CD_3)_2SO$, 25°C): δ 7.35 (s, 2H, C*H*$_{Im\text{-}4,5}$), 7.04 (s, 4H, C*H*$_{Mes}$), 3.94 (s, 5H, Cp), 2.32 (s, 6H, C*H*$_{3para\text{-}Mes}$), 2.02 (s, 12H, C*H*$_{3ortho\text{-}Mes}$); ^{13}C{^{1}H} NMR (100.6 MHz, C_6D_6, 25°C): δ 234.4 (Mn–*C*O), 205.4 (Mn–*C*N$_2$), 138.6 (*C*–CH$_{3para\text{-}Mes}$), 138.5 (C$_{ipso\text{-}Mes}$), 136.3 (*C*–CH$_{3ortho\text{-}Mes}$), 129.4 (*C*H$_{Mes}$), 123.8 (*C*H$_{Im\text{-}4,5}$), 81.5 (Cp), 21.2 (*C*H$_{3para\text{-}Mes}$), 18.5 (*C*H$_{3ortho\text{-}Mes}$); ^{13}C{^{1}H} NMR (100.6 MHz, $(CD_3)_2SO$, 25°C): δ 233.9 (Mn–*C*O), 200.2 (Mn–*C*N$_2$), 137.8 (C$_{ipso\text{-}Mes}$), 137.6 (*C*–CH$_{3para\text{-}Mes}$), 135.5 (*C*–CH$_{3ortho\text{-}Mes}$), 128.6 (*C*H$_{Mes}$), 124.9 (*C*H$_{Im\text{-}4,5}$), 81.1 (Cp), 20.7 (*C*H$_{3para\text{-}Mes}$), 17.8 (*C*H$_{3ortho\text{-}Mes}$); IR (Et_2O): ν_{CO} 1918 (s), 1852 (s) cm^{-1}.

Generation of complex (η^5-C$_5$H$_5$)(CO)$_2$Mn(IMesLi) ([2]Li×3THF) for NMR characterization. To a yellow solution of complex **1** (38 mg, 0.079 mmol) in THF (2 mL) a solution of *n*-BuLi (63 μL of 1.6M in hexane, 0.10 mmol) was added dropwise at room temperature. The reaction mixture rapidly turned orange, the solution was stirred at room temperature for 10 min and then evaporated under vacuum. The orange residue was dissolved in dry C_6D_6 (0.8 mL) and the resulting solution was filtered under nitrogen directly to NMR tube through a plug of glass wool in the Pasteur pipette to provide a suitable sample of [**2**]Li×3THF containing based on ^{1}H spectra three THF molecules solvating lithium atom and *ca.* 10% of complex **1**.

[**2**]Li×3THF: ^{1}H NMR (400.1 MHz, C_6D_6, 25°C): δ 7.05 (s, 2H, C*H*$_{Mes}$), 6.96 (s, 2H, C*H*$_{Mes}$), 6.55 (br s, 1H, C*H*$_{Im\text{-}4}$), 4.22 (s, 5H, Cp), 3.43 (very br s, 12H, CH$_2$C*H*$_2$O$_{THF}$), 2.32, 2.28, 2.24, (overlapped s, 18H, C*H*$_{3ortho\text{-}Mes}$ + C*H*$_{3para\text{-}Mes}$), 1.38 (br s, 12H, C*H*$_2$CH$_2$O$_{THF}$); ^{13}C{^{1}H} NMR (100.6 MHz, C_6D_6, 25°C): δ 236.8 (Mn–*C*O), 191.1 (Mn–*C*N$_2$), 171.2 (*C*–Li), 146.3, 140.9 (C$_{ipso\text{-}Mes}$), 136.7, 136.5 (*C*–CH$_{3ortho\text{-}Mes}$), 136.6, 135.2 (*C*–CH$_{3para\text{-}Mes}$), 132.0 (*C*H$_{Im\text{-}4}$), 129.0, 128.7 (*C*H$_{Mes}$), 82.2 (Cp), 69.0 (very br s, CH$_2$*C*H$_2$O$_{THF}$), 25.9 (br s, *C*H$_2$CH$_2$O$_{THF}$), 21.3, 21.2 (*C*H$_{3para\text{-}Mes}$), 19.3, 18.9 (*C*H$_{3ortho\text{-}Mes}$); ^{7}Li NMR (155.5 MHz, C_6D_6, 25°C): δ 0.5.

Synthesis of (η^5-C$_5$H$_5$)(CO)$_2$Mn(IMesCOOH) (3). To a yellow suspension of complex **1** (1.71 g, 3.55 mmol) in ether (100 mL) a 1.6M solution of *n*-BuLi in hexane (2.55 mL, 4.08 mmol) was added dropwise at room temperature under stirring. The precipitate of **1** gradually dissolved and the resulting deep orange solution of complex [**2**]Li (ν_{CO} 1905 (s), 1837 (s) cm^{-1}) was additionally stirred for *ca.* 1 h and then a stream of dry CO_2 was passed for several minutes

through the solution to form an abundant yellow precipitate of (η^5-C_5H_5)$(CO)_2$Mn(IMesCOOLi). After stirring the reaction mixture for *ca.* 30 min a 2M solution of HCl in ether (2.5 mL, 5.00 mmol) was added leading to the formation of a yellow solution of complex **3** as evidenced by IR spectroscopy (ν_{CO} 1922 (s), 1856 (s) cm^{-1}, ν_{COOH} 1736 cm^{-1} (m br.)). The reaction mixture was evaporated under vacuum and the orange residue was purified by chromatography on a silica column (2×15 cm). Elution with dichloromethane afforded a yellow band containing some unreacted complex **1** (140 mg), followed by a yellow-orange band of the product **3** eluted with 1:1 CH_2Cl_2/ether mixture. The eluate was evaporated under vacuum and the residue was recrystallized in CH_2Cl_2/hexane at –20°C to give complex **3** (1.58 g, 85% yield) as orange crystals. Single crystals of **3** suitable for an X-ray diffraction study were obtained by the crystallization from benzene solution at 5° C.

3: ^{1}H NMR (400.1 MHz, $(CD_3)_2SO$, 25°C): δ 13.05 (very br s, 1H, COO*H*), 7.91 (br s, 1H, C*H*$_{Im\text{-}4}$), 7.05 (s, 2H, C*H*$_{Mes}$), 6.96 (br s, 2H, C*H*$_{Mes}$), 3.94 (s, 5H, Cp), 2.32 (s, 6H, C*H*$_{3para\text{-}Mes}$), 2.01 (s, 6H, C*H*$_{3ortho\text{-}Mes}$), 1.94 (br s, 6H, C*H*$_{3ortho\text{-}Mes}$); $^{13}C\{^1H\}$ NMR (100.6 MHz, $(CD_3)_2SO$, 25°C): δ 233.3 (Mn–*C*O), 208.7 (Mn–*C*N_2), 158.4 (*C*OOH), 137.9, 137.3 (*C*–$CH_{3para\text{-}Mes}$), 137.0, 136.8 ($C_{ipso\text{-}Mes}$), 135.8, 135.4 (*C*–$CH_{3ortho\text{-}Mes}$), 130.9 ($CH_{Im\text{-}4}$), 128.7, 128.3 (*C*H_{Mes}), 81.3 (Cp), 20.8, 20.7 (*C*$H_{3para\text{-}Mes}$), 18.0, 17.9 (*C*$H_{3ortho\text{-}Mes}$); IR (Et_2O): ν_{CO} 1922 (s), 1856 (s) cm^{-1}, $\nu_{CO(OH)}$ 1736 cm^{-1} (m br.); Anal. Found: C, 66.71; H, 5.62; N, 5.06; Calcd. for $C_{29}H_{29}MnN_2O_4$: C, 66.41; H, 5.57; N, 5.34.

Synthesis of complex $Phen_2Cu_3(\mu_2$-(OOCIMes)$Mn(CO)_2Cp)_4(\mu_2$-$OAc)_2$ (4). To a solution of (1,10-Phen)$Cu(OAc)_2$ (73 mg, 0.219 mmol) in MeCN (20 mL) a solution of **3** (136 mg, 0.259 mmol) in MeCN (20 mL) was added under stirring at RT. IR monitoring showed almost instantaneous transformation of ν_{CO} bands of **3** (1912 (s), 1841 (s) cm^{-1}) into those of complex **4** (1909 (s), 1838 (s) cm^{-1}) as well as the disappearance of $\nu_{CO(OH)}$ band of **3** at 1736 cm^{-1} and the appearance of new $\nu_{CO(OH)}$ bands (1754 and 1725 cm^{-1}) attributed to the acetic acid. The resulting deep-green solution was stirred for 15 min at room temperature, filtered through Celite, concentrated to *ca.* 7 mL and left to stand for 4-6 hours at room temperature to form green crystals of **4**, some of them were suitable for X-ray diffraction experiment. The supernatant was removed by decantation

and the product was washed with ether (10 mL) and dried under vacuum to give complex **4** (125 mg, 83%) as green crystals.

4: IR (MeCN): 1909 (s), 1838 (s) ν_{CO}, 1630-1550 (m) $\nu_{CO(O)}$ + $\nu_{C=C}$; X-band ESR (9.51 GHz, 1:1 CH_2Cl_2/toluene glass, 120K): $g_{1||}$ = 2.282 ($A_{1||}$ = 150 G), $g_{1\perp}$ = 2.060 ($A_{1\perp}$ = 13 G); g_2 = 2.018 (a_2 = 166 G); μ_{eff} (CD_2Cl_2, 25°C) = 3.93 μ_B; Anal. Found: C, 60.87; H, 4.64; N, 6.84 (average of two samples). Calc. for $C_{148}H_{140}Cu_3Mn_4N_{14}O_{20}$ (**4**×2MeCN, four solvate MeCN molecules lost): 62.48; H, 4.96; N, 6.89. The analytical data were found to be reproducibly low in carbon probably due to the formation of metal carbides.[8]

Synthesis of complex $Phen_2Zn_3(\mu_2\text{-}(OOCIMes)Mn(CO)_2Cp)_4(\mu_2\text{-}OAc)_2$ (5). To a solution of (1,10-Phen)$Zn(OAc)_2$ (73 mg, 0.217 mmol) in MeCN (10 mL) a solution of **3** (136 mg, 0.259 mmol) in MeCN (10 mL) was added under stirring at RT. IR monitoring showed almost instantaneous transformation of ν_{CO} bands of **3** (1912 (s), 1841 (s) cm^{-1}) into those of complex **5** (1909 (s), 1838 (s) cm^{-1}) as well as the disappearance of $\nu_{CO(OH)}$ band of **3** at 1736 cm^{-1} and the appearance of new $\nu_{CO(OH)}$ bands (1754 and 1725 cm^{-1}) attributed to the acetic acid. The resulting yellow solution was stirred for 15 min at room temperature, filtered through Celite, concentrated to *ca.* 10 mL and kept at 5° C over 24h to form yellow crystals of **5**, some of them were suitable for X-ray diffraction experiment. The supernatant was removed by decantation and the product was washed with ether (10 mL) and dried under vacuum to give complex **5** (98 mg, 65%) as transparent yellow crystals.

5: ^{1}H NMR (400.1 MHz, CD_2Cl_2, 25° C): 9.20-7.40 (br m, 16H, phen), 7.01 (br. s, 8H, CH_{Mes}), 3.88 (br s, 20H, Cp), 2.70-0.70 (overlapped br s, 96H, CH_{3Mes} + CH_3COO + CH_3CN solvate); IR (MeCN): 1909 (s), 1838 (s) ν_{CO}, 1630-1550 (m) $\nu_{CO(O)}$ + $\nu_{C=C}$; Anal. Found: C, 61.34; H, 4.65; N, 7.36 (average of three samples). Calc. for $C_{150}H_{143}Mn_4N_{15}O_{20}Zn_3$ (**5**×3MeCN, three solvate MeCN molecules lost): C, 62.30; H, 4.98; N, 7.27. The analytical data were found to be reproducibly low in carbon probably due to the formation of metal carbides.[8]

X-ray diffraction studies. Single-crystal X-ray diffraction data collections were carried out on a Bruker SMART / APEX II diffractometer (graphite monochromator, Mo Kα radiation, λ = 0.71073 Å). All calculations were performed on a PC compatible computer using the WinGX system.[9] The structures were solved using the SIR92 program,[10] which revealed in each instance the position of most of the non-hydrogen atoms. All the remaining non-hydrogen atoms were located by the usual combination of full matrix least-squares refinement and difference electron density syntheses using the SHELX program.[11] Atomic scattering factors were taken from the usual tabulations. Anomalous dispersion terms for the Mn, Cu, and Zn atoms were included in Fc. All non-hydrogen atoms were allowed to vibrate anisotropically. The hydrogen atoms were generally set in idealized positions (R_3CH, C–H = 0.96 Å; R_2CH_2, C–H = 0.97 Å; RCH_3, C–H = 0.98 Å; C(sp^2)–H = 0.93 Å; U_{iso} 1.2 or 1.5 times greater than the Ueq of the carbon atom to which the hydrogen atom is attached) and their positions refined as "riding" atoms except for H4 in the structure of **3**, whose position was inferred from a residual electron density map and refined with a U_{iso} arbitrarily set at 0.04 $Å^2$. CCDC 1481172-1481174 contain the supplementary crystallographic data for the three structures unveiled in this paper. These data can be obtained free of charge from the Cambridge Crystallographic Data Centre via www.ccdc.cam.ac.uk/data_request/cif.

Figure 1S. A prespective view of one of the four independent molecules of complex **1** (ellipsoids are show at the 30% probability level). Selected averaged bond lengths (Å): Mn1–C1 1.767[2]; Mn1–C2 1.761[3]; Mn1–C3 2.003[3]; C3-N1 1.366[1]; C3-N2 1.374[2]; N1-C4 1.387[1]; N2-C5 1.391[2]; C4-C5 1.339[2], where the value between brakets represent the *esd* in the averaged bond length $\bar{l}$ given by the equation [σ] = $\sqrt{\sum_{n=1}^{4}(l_n-\bar{l})^2/n(n-1)}$. The structure of complex **1** is available from the CCDC under the reference number CCDC-1485213.

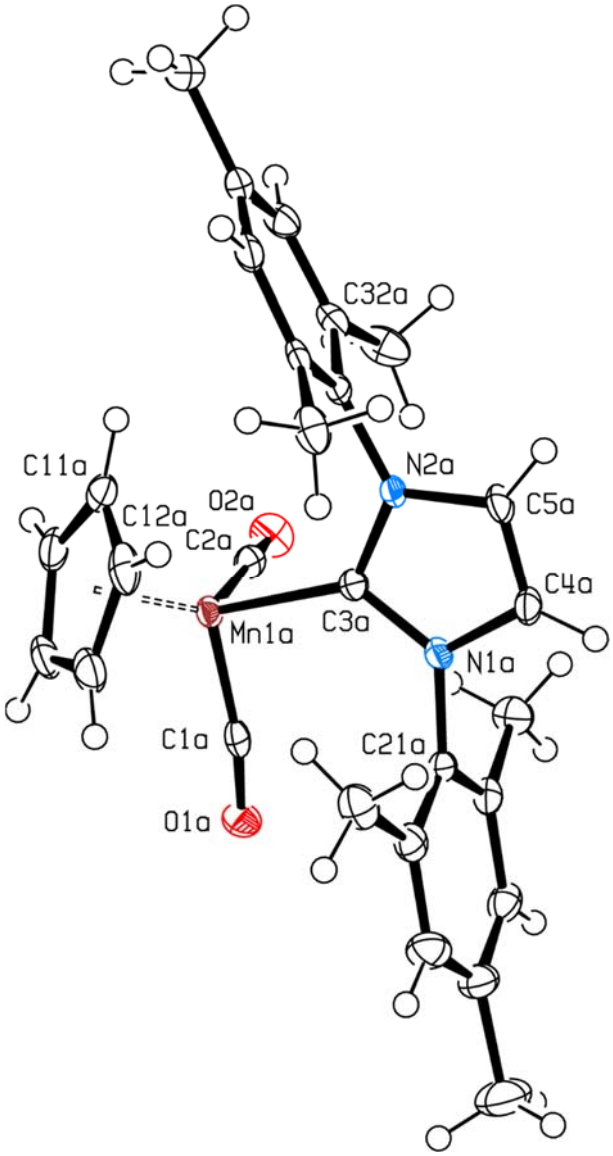

Table 1S. Crystal data and structure refinements for **3**, **4**, and **5**

Complex	**3**•C_6H_6	**4**•6(C_2H_3N)	**5**•6(C_2H_3N)
empirical formula	$C_{29}H_{29}MnN_2O_4$,C_6H_6	$C_{144}H_{134}Cu_3Mn_4N_{12}O_{20}$,6($C_2H_3N$)	$C_{144}H_{134}Mn_4N_{12}O_{20}Zn_3$,6($C_2H_3N$)
M_r	602.59	3009.37	3014.82
T/ K	150	100	150
λ /Å	0.71069	0.71069	0.71069
Crystal system	tetragonal	triclinic	triclinic
Space group (no.)	$I4_1/a$ (#88)	P1(bar) (#2)	P1(bar) (#2)
a/ Å	18.0191(6)	13.3188(8)	13.3746(9)
b/ Å	18.0191(6)	16.5533(9)	16.7199(11)
c/ Å	37.650(3)	17.9688(11)	18.0349(12)
α/ °	90	104.502(2)	104.6490(10)
β/ °	90	102.667(2)	102.7660(10)
γ/ °	90	101.546(2)	101.6240(10)
V/ Å^3	12224.5(13)	3603.0(4)	3661.2(4)
Z	16	1	1
D_c/ g.cm^{-3}	1.310	1.387	1.367
μ/ mm^{-1}	0.473	0.847	0.889
F(000)	5056	1561	1564
θ_{max}/ °	30.0	29.0	28.0
Completeness to θ_{max} (%)	0.99	0.99	0.99
Index range, *hkl*	-18<h<25	-17<h<17	-17<h<17
	-25<k<14	-27<k<22	-21<k<22
	-51<l<52	-23<l<23	-23<l<23
Reflections collected	31624	150778	37766

Table 1S (continued)

Independent reflections	8862	19080	17534
Parameters	390	917	917
GOF	1.03	1.02	1.03
R [I>2σ(I)]	0.0404	0.0528	0.0487
R_w [I>2σ(I)]	0.1002	0.1232	0.0746
R (all data)	0.0607	0.1027	0.1243
Rw (all data)	0.1131	0.1484	0.1390
$\Delta\rho_{max/min}$/ e.Å^{-3}	-0.29/0.37	-2.109/0.924	-2.206/0.996

Table 2S. Selected bond distances and angles for complex **3**

Bond Distances (Angstrom)

Mn1 -C1	1.7710(18)
Mn1 -C2	1.7734(18)
Mn1 -C3	1.9808(15)
O1 -C1	1.163(2)
O2 -C2	1.165(2)
O3 -C6	1.2226(19)
O4 -C6	1.3187(18)
N1 -C3	1.3825(18)
N1 -C4	1.3977(18)
N1 -C21	1.4495(19)
N2 -C3	1.3887(19)
N2 -C5	1.3755(19)
N2 -C31	1.4453(19)
C4 -C6	1.462(2)
C4 -C5	1.345(2)

Bond Angles (degree)

C1 -Mn1 -C2	91.81(9)
C1 -Mn1 -C3	94.58(7)
C2 -Mn1 -C3	98.78(7)
C3 -N1 -C4	111.46(12)
C3 -N2 -C5	112.34(12)
Mn1 -C1 -O1	175.46(15)
Mn1 -C2 -O2	171.37(17)
Mn1 -C3 -N2	128.55(10)
N1 -C3 -N2	102.18(12)
Mn1 -C3 -N1	129.08(11)
N1 -C4 -C5	106.96(13)
C5 -C4 -C6	127.28(14)
N1 -C4 -C6	125.49(13)
N2 -C5 -C4	107.05(13)
O3 -C6 -C4	123.21(14)
O4 -C6 -C4	111.69(13)
O3 -C6 -O4	125.09(14)

Figure 2S. A perspective view of dimer complex **3** (ellipsoids are show at the 30% probability level).

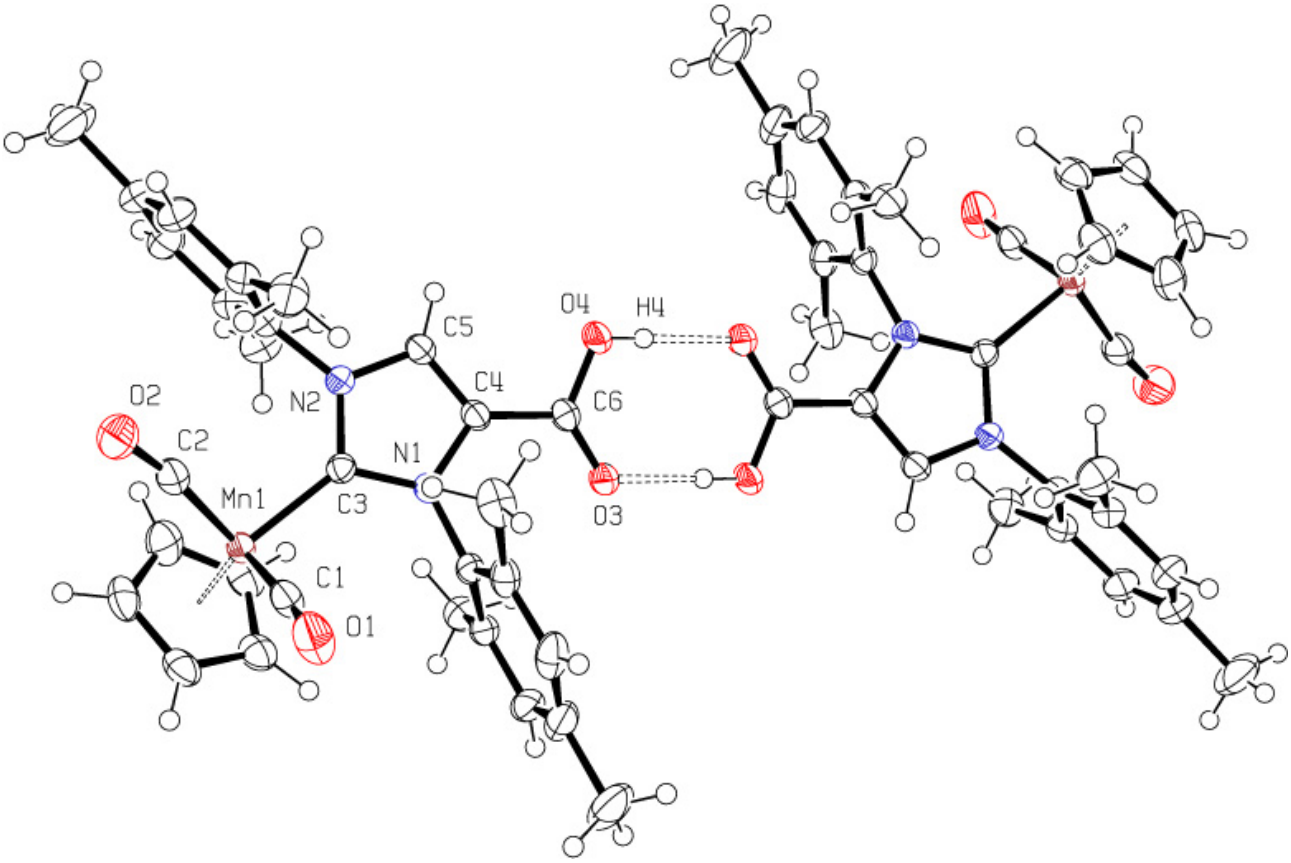

Table 3S. Selected bond distances and angles for complex **4**

Bond Distances (Angstrom)

Cu1	-O6	2.187(2)
Cu1	-O31	2.1808(19)
Cu1	-O32	2.1670(18)
Cu1	-O6_a	2.187(2)
Cu1	-O31_a	2.1807(19)
Cu1	-O32_a	2.1670(18)
Cu2	-O5	2.669(3)
Cu2	-O6	1.9915(19)
Cu2	-O41	1.948(2)
Cu2	-O42	2.160(2)
Cu2	-N3	2.039(3)
Cu2	-N4	2.030(3)

a = 1-x,1-y,-z

Bond Angles (degree)

O6	-Cu1	-O31	85.81(8)
O6	-Cu1	-O32	87.53(7)
O6	-Cu1	-O6_a	180.00
O6	-Cu1	-O31_a	94.19(8)
O6	-Cu1	-O32_a	92.47(7)
O31	-Cu1	-O32	92.47(7)
O6_a	-Cu1	-O31	94.19(8)
O31	-Cu1	-O31_a	180.00
O31	-Cu1	-O32_a	87.53(7)
O6_a	-Cu1	-O32	92.47(7)
O31_a	-Cu1	-O32	87.53(7)
O32	-Cu1	-O32_a	180.00
O6_a	-Cu1	-O31_a	85.81(8)
O6_a	-Cu1	-O32_a	87.53(7)
O31_a	-Cu1	-O32_a	92.47(7)
O5	-Cu2	-O6	54.10(8)
O5	-Cu2	-O41	91.79(9)
O5	-Cu2	-O42	155.84(8)
O5	-Cu2	-N3	108.38(10)
O5	-Cu2	-N4	86.59(10)

Table 3S (continued)

O6	-Cu2	-O41	92.99(9)
O6	-Cu2	-O42	103.36(8)
O6	-Cu2	-N3	161.91(10)
O6	-Cu2	-N4	92.60(9)
O41	-Cu2	-O42	98.65(9)
O41	-Cu2	-N3	92.01(10)
O41	-Cu2	-N4	171.76(9)
O42	-Cu2	-N3	93.07(9)
O42	-Cu2	-N4	85.93(9)
N3	-Cu2	-N4	80.87(10)

a = 1-x,1-y,-z

Figure 3S. A perspective view of complex **4** showing all atoms (ellipsoids are show at the 30% probability level).

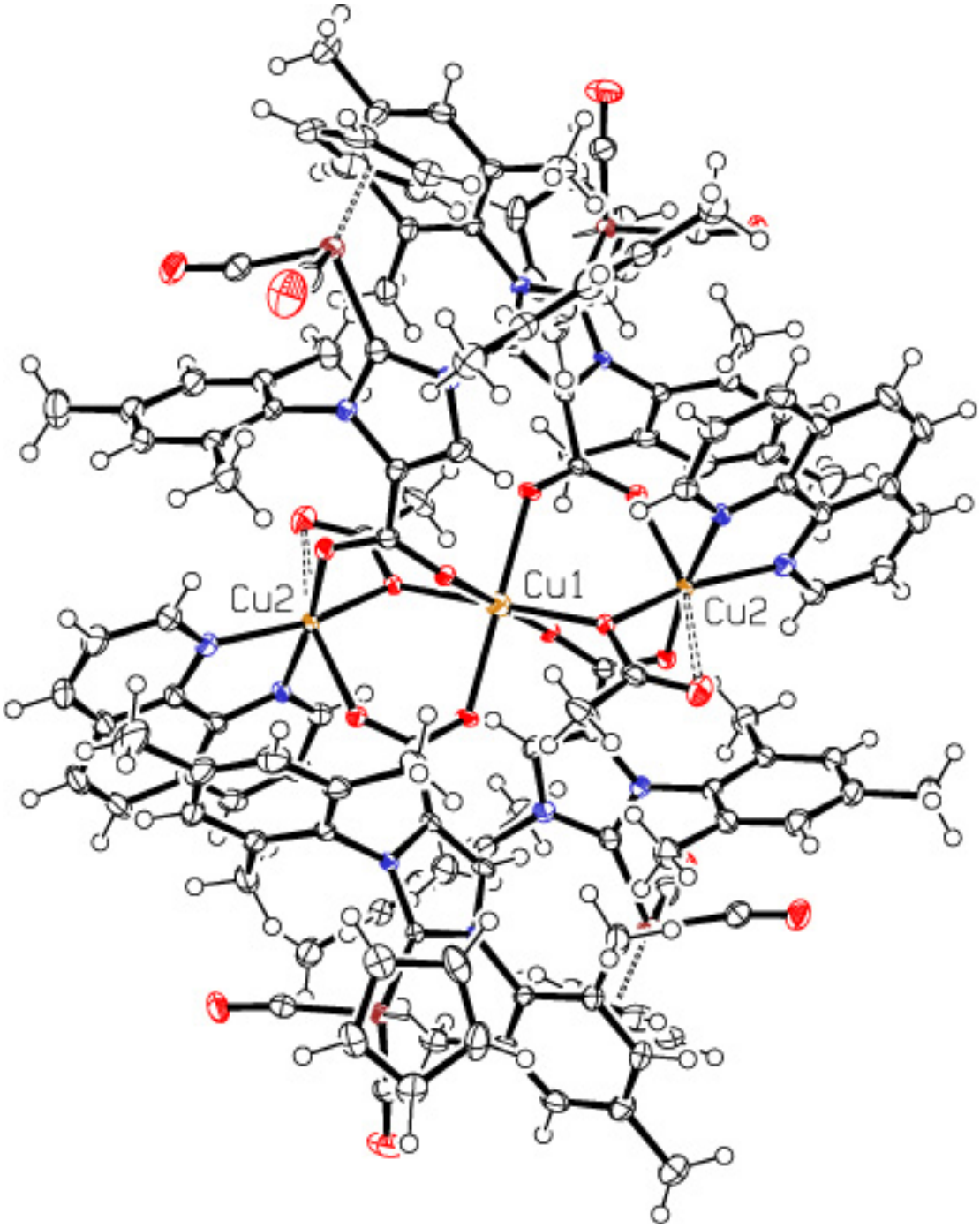

Table 4S. Selected bond distances and angles for complex **4**

Bond Distances (Angstrom)

Zn1	-O6	2.133(2)
Zn1	-O31	2.1772(19)
Zn1	-O32	2.1623(19)
Zn1	-O6_a	2.1331(19)
Zn1	-O31_a	2.1772(19)
Zn1	-O32_a	2.1624(19)
Zn2	-O5	2.408(3)
Zn2	-O6	2.0839(19)
Zn2	-O41	2.0195(19)
Zn2	-O42	2.0267(19)
Zn2	-N3	2.1131(19)
Zn2	-N4	2.175(2)

a = 1-x,1-y,-z

Bond Angles (degree)

O6	-Zn1	-O31	87.63(7)
O6	-Zn1	-O32	87.51(7)
O6	-Zn1	-O6_a	180.00
O6	-Zn1	-O31_a	92.37(7)
O6	-Zn1	-O32_a	92.49(7)
O31	-Zn1	-O32	92.10(7)
O6_a	-Zn1	-O31	92.37(7)
O31	-Zn1	-O31_a	180.00
O31	-Zn1	-O32_a	87.90(7)
O6_a	-Zn1	-O32	92.49(7)
O31_a	-Zn1	-O32	87.90(7)
O32	-Zn1	-O32_a	180.00
O6_a	-Zn1	-O31_a	87.62(7)
O6_a	-Zn1	-O32_a	87.51(7)
O31_a	-Zn1	-O32_a	92.10(7)
O5	-Zn2	-O6	57.64(8)
O5	-Zn2	-O41	89.24(9)
O5	-Zn2	-O42	159.57(8)
O5	-Zn2	-N3	99.98(9)
O5	-Zn2	-N4	86.79(9)

Table 4S (continued)

O6	-Zn2	-O41	95.23(8)
O6	-Zn2	-O42	103.10(8)
O6	-Zn2	-N3	155.87(9)
O6	-Zn2	-N4	91.40(8)
O41	-Zn2	-O42	100.10(8)
O41	-Zn2	-N3	93.19(9)
O42	-Zn2	-N3	97.61(8)
O42	-Zn2	-N4	87.01(8)
N3	-Zn2	-N4	77.33(9)

a = 1-x, 1-y, -z

Figure 4S. A perspective view of complex **5** showing all atoms (ellipsoids are show at the 30% probability level).

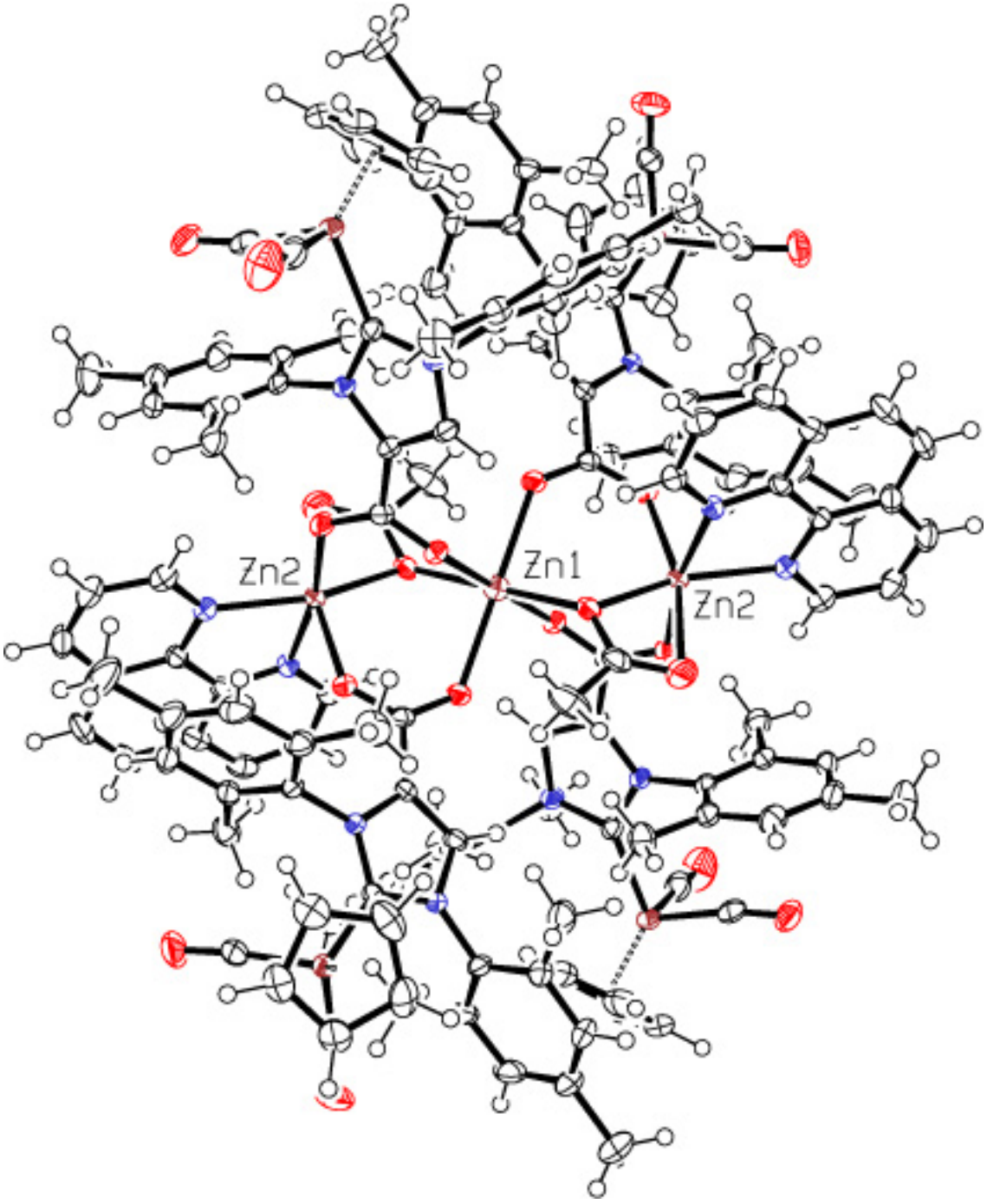

References:

1 L. Hintermann, *Beilstein J. Org. Chem.*, 2007, **3**, 22.

2 M. Devereux, D. O'Shea, M. O'Connor, H. Grehan, G. Connor, M. McCann, G. Rosair, F. Lyng, A. Kellett, M. Walsh, D. Egan and B. Thati, *Polyhedron*, 2007, **26**, 4073.

3 M. A. Uvarova, M. A. Kushan and S. E. Nefedov, *Russ. J. Inorg. Chem.*, 2012, **57**, 515.

4 G. R. Fulmer, A. J. M. Miller, N. H. Sherden, H. E. Gottlieb, A. Nudelman, B. M. Stoltz, J. E. Bercaw and K. I. Goldberg, *Organometallics*, 2010, **29**, 2176.

5 S. Stoll and A. Scheweiger, *J. Magn. Reson.* 2006, **178**, 42.

6 G. A. Bain and J. F. Berry, *J. Chem. Educ.*, 2008, **85**, 532.

7 J. Zheng, S. Elongovan, D. A. Valyaev, R. Brousses, V. César, J.-B. Sortais, C. Darcel, N. Lugan and G. Lavigne, *Adv. Synth. Catal.*, 2014, **356**, 1093.

8 R. A. Musgrave, R. S. P. Turbervill, M. Irwin and J. M. Goicoechea, *Angew. Chem. Int. Ed.*, 2012, **51**, 10832.

9 L. J. Farrugia, *J. Appl. Cryst.,* 1999, **32**, 837.

10 A. Altomare, G. Cascarano, C. Giacovazzo and A. Guagliardi, *J. Appl. Cryst.,* 1994, **27**, 435.

11 G. M. Sheldrick, *Acta Cryst.,* 2008, **A64**, 112.

Figure 5S. ^{1}H NMR spectrum of complex **1** (400.1 MHz, C_6D_6, 25°C)

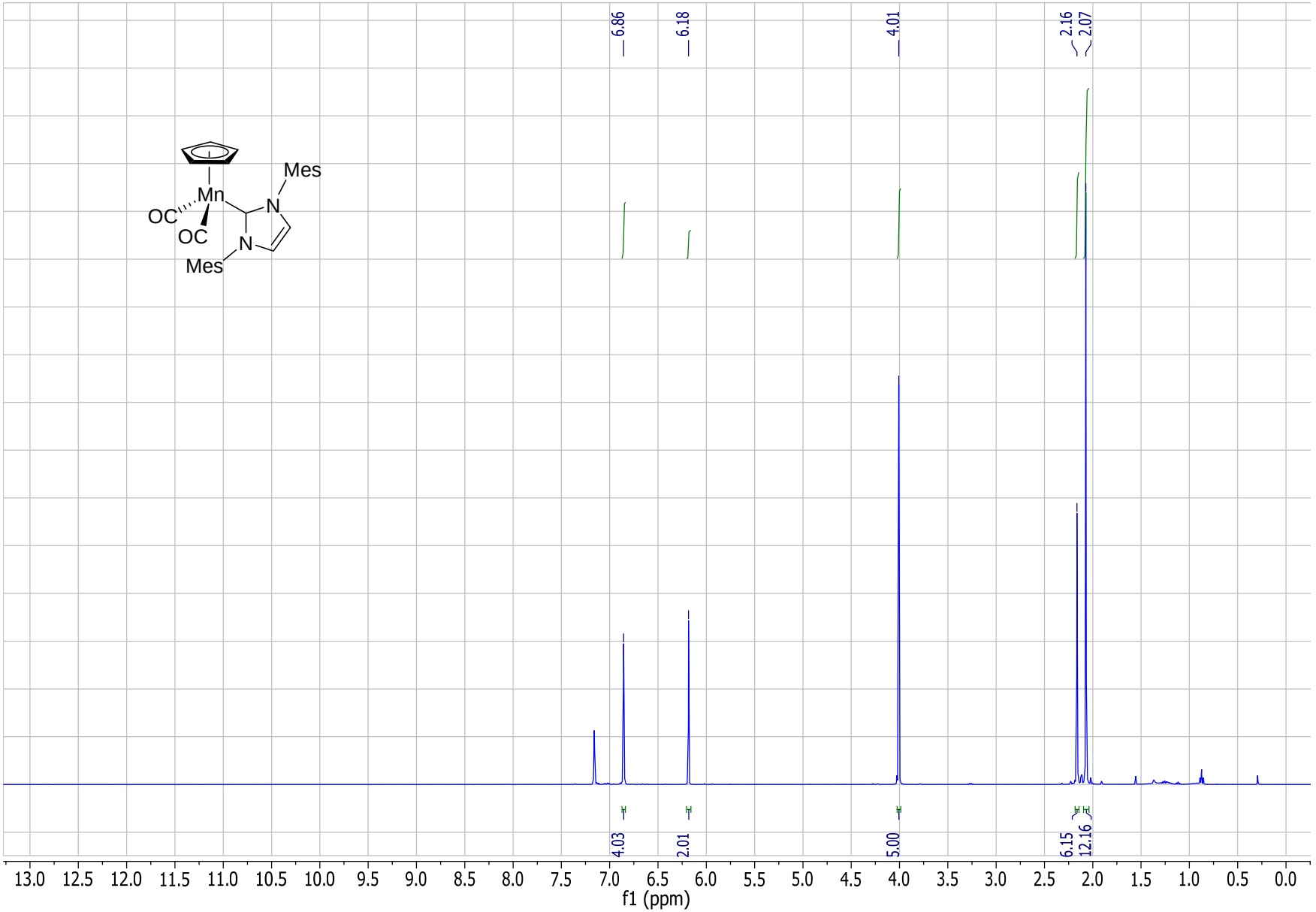

Figure 6S. $^{13}C\{^{1}H\}$ NMR spectrum of complex **1** (100.6 MHz, C_6D_6, 25°C)

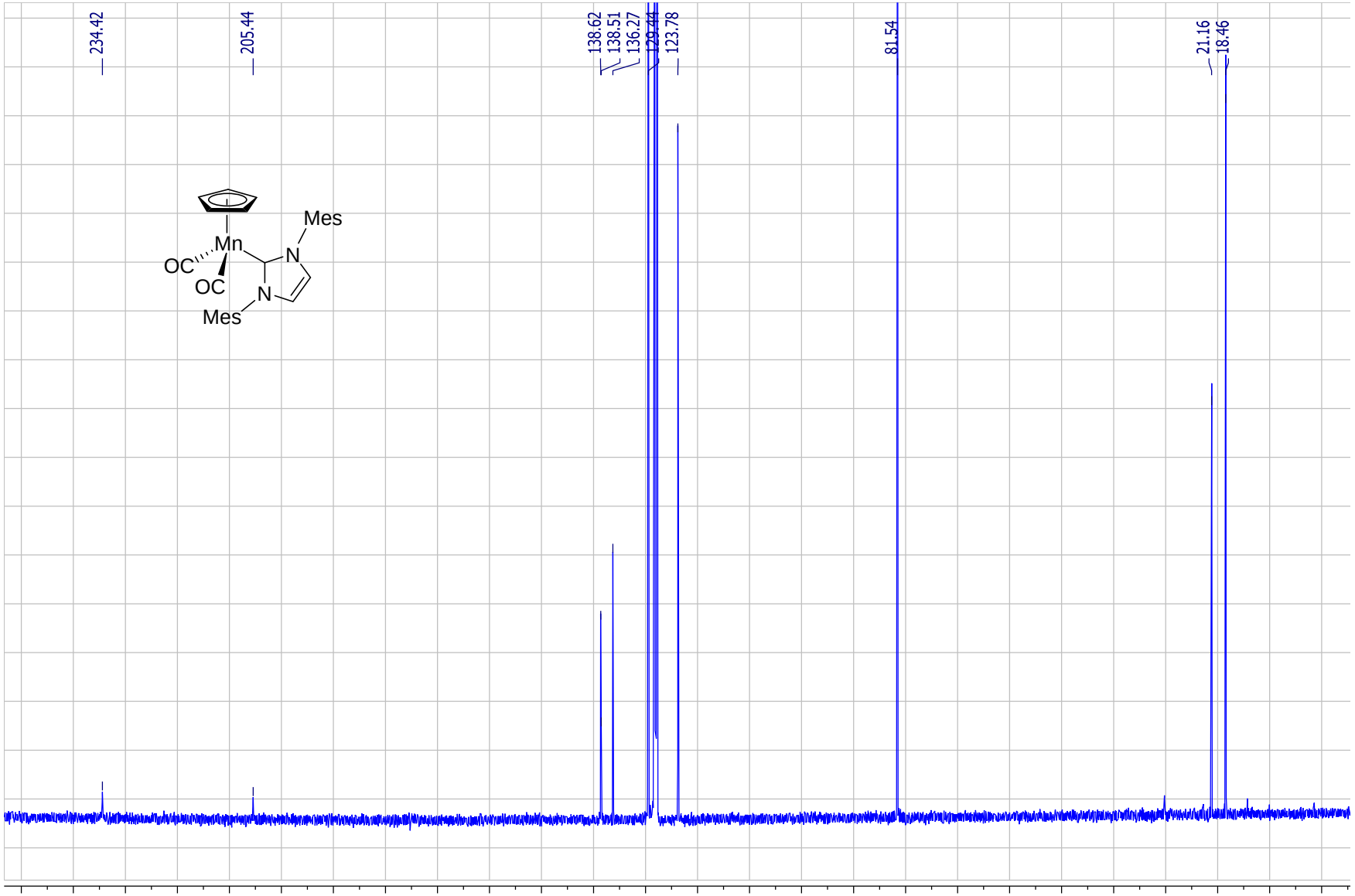

Figure 7S. ^{1}H NMR spectrum of complex **1** (400.1 MHz, $(CD_3)_2SO$, 25°C), the peak of residual water is marked with asterisk

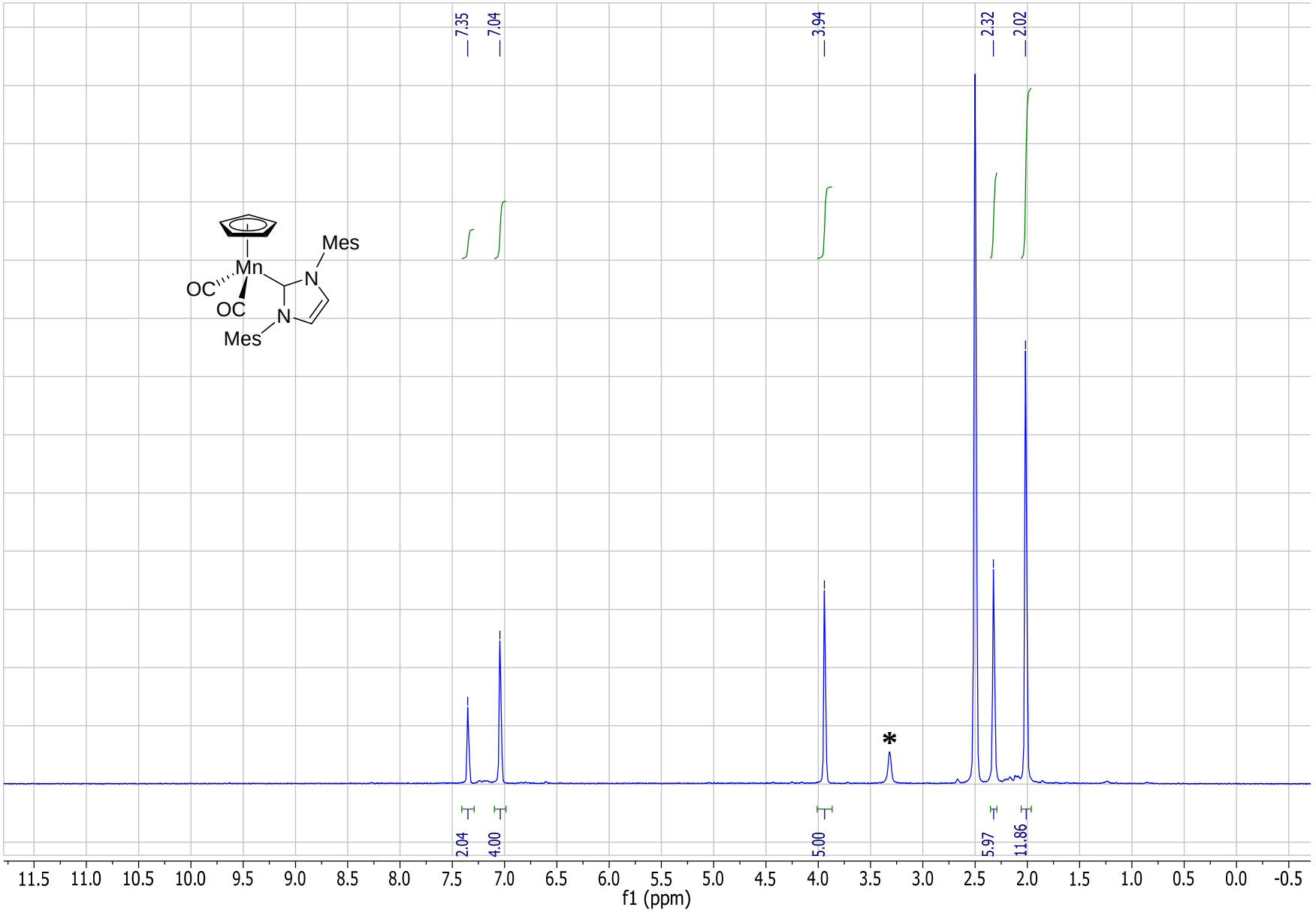

Figure 8S. $^{13}C\{^{1}H\}$ NMR spectrum of complex **1** (100.6 MHz, $(CD_3)_2SO$, 25°C)

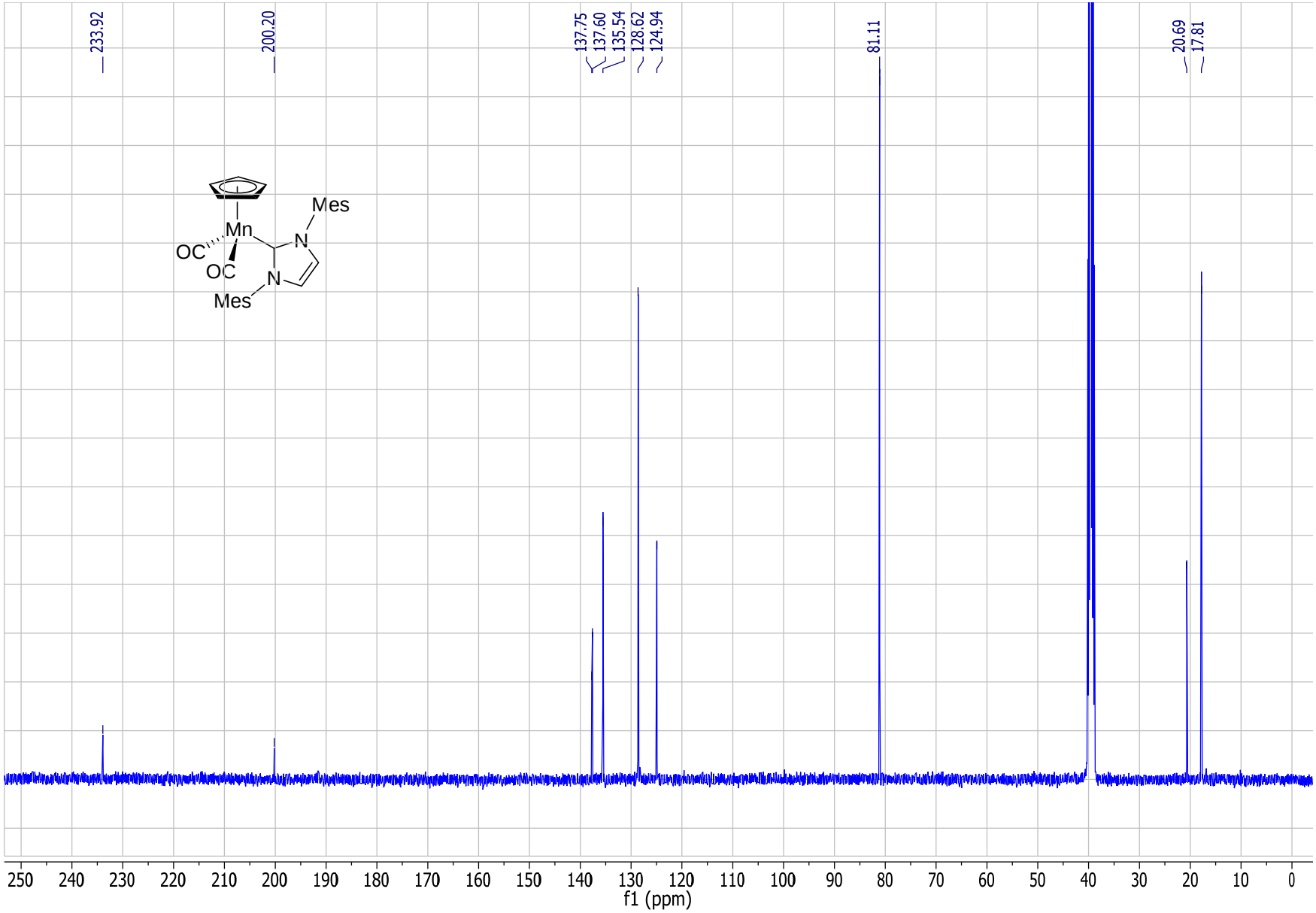

Figure 9S. ^{1}H NMR spectrum of complex [**2**]Li×3THF (400.1 MHz, C_6D_6, 25°C), the peaks of the starting complex **1** are marked with asterisk

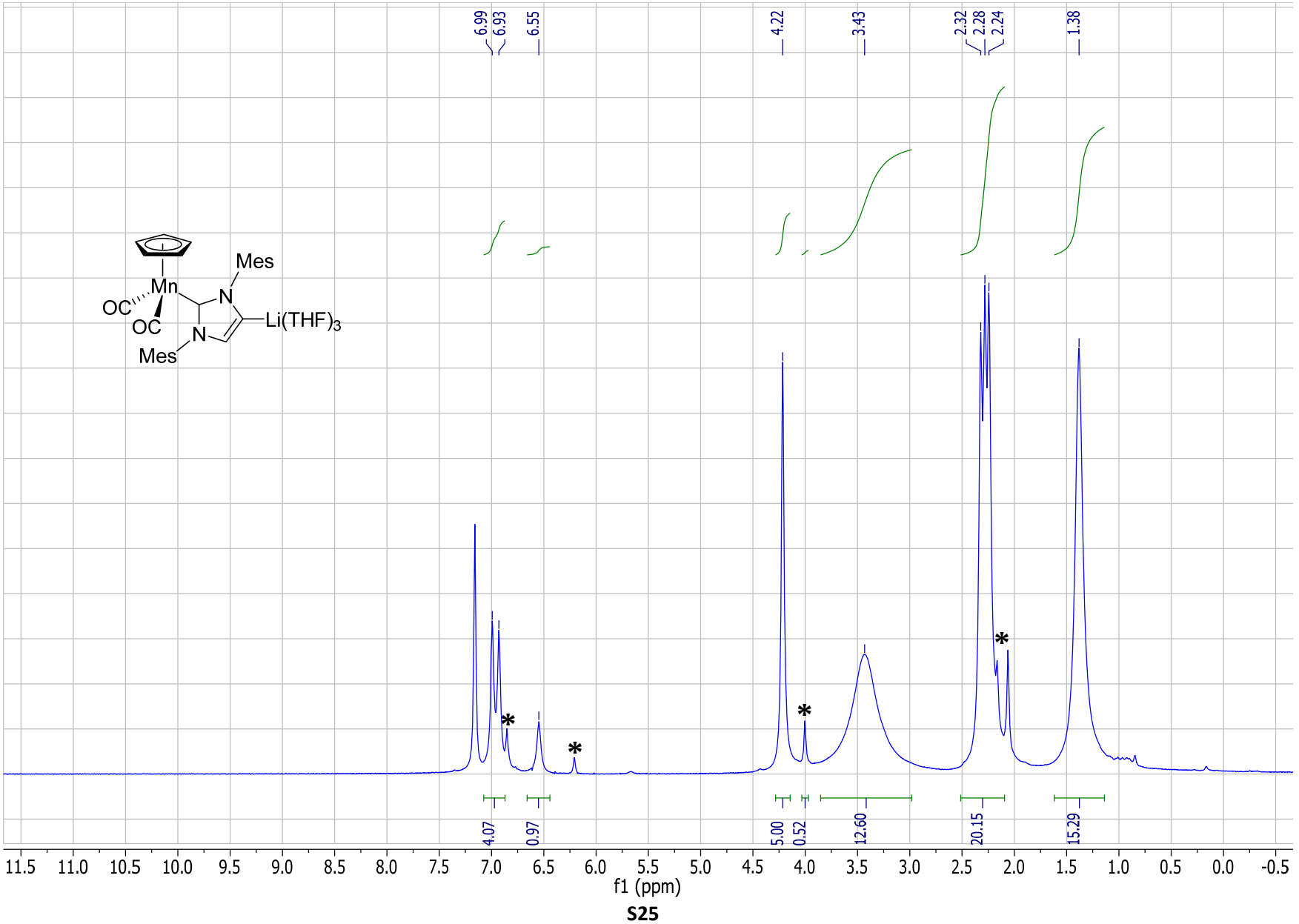

Figure 10S. $^{13}C\{^{1}H\}$ NMR spectrum of complex [**2**]Li×3THF (100.6 MHz, C_6D_6, 25°C), the peaks of residual complex **1** are marked with asterisk

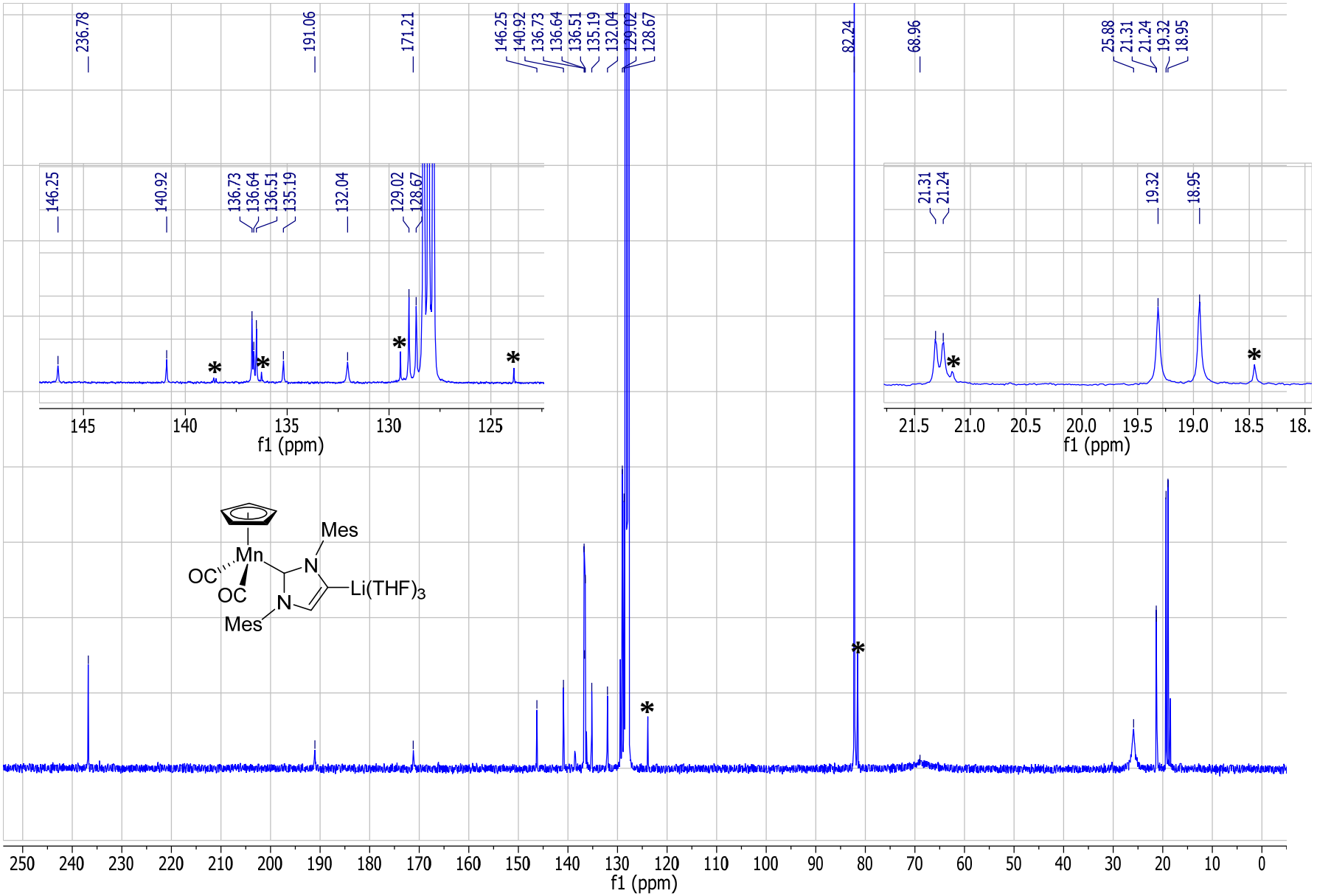

Figure 11S. $^{13}C\{^{1}H\}$ JMOD NMR spectrum of complex [**2**]Li×3THF (100.6 MHz, C_6D_6, 25°C), the peaks of residual complex **1** are marked with asterisk

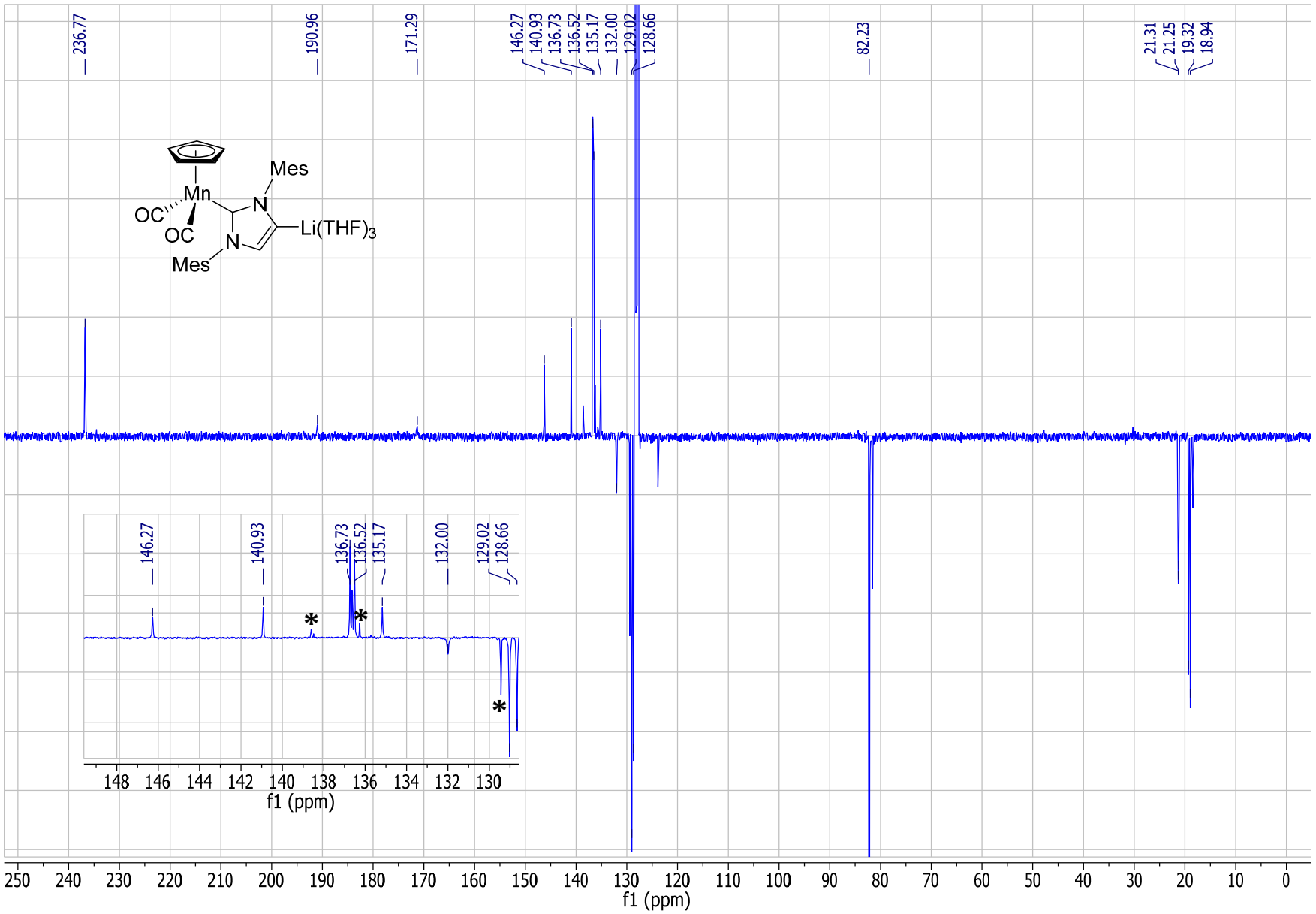

Figure 12S. ^{7}Li NMR spectrum of complex [**2**]Li×3THF (155.5 MHz, C_6D_6, 25°C)

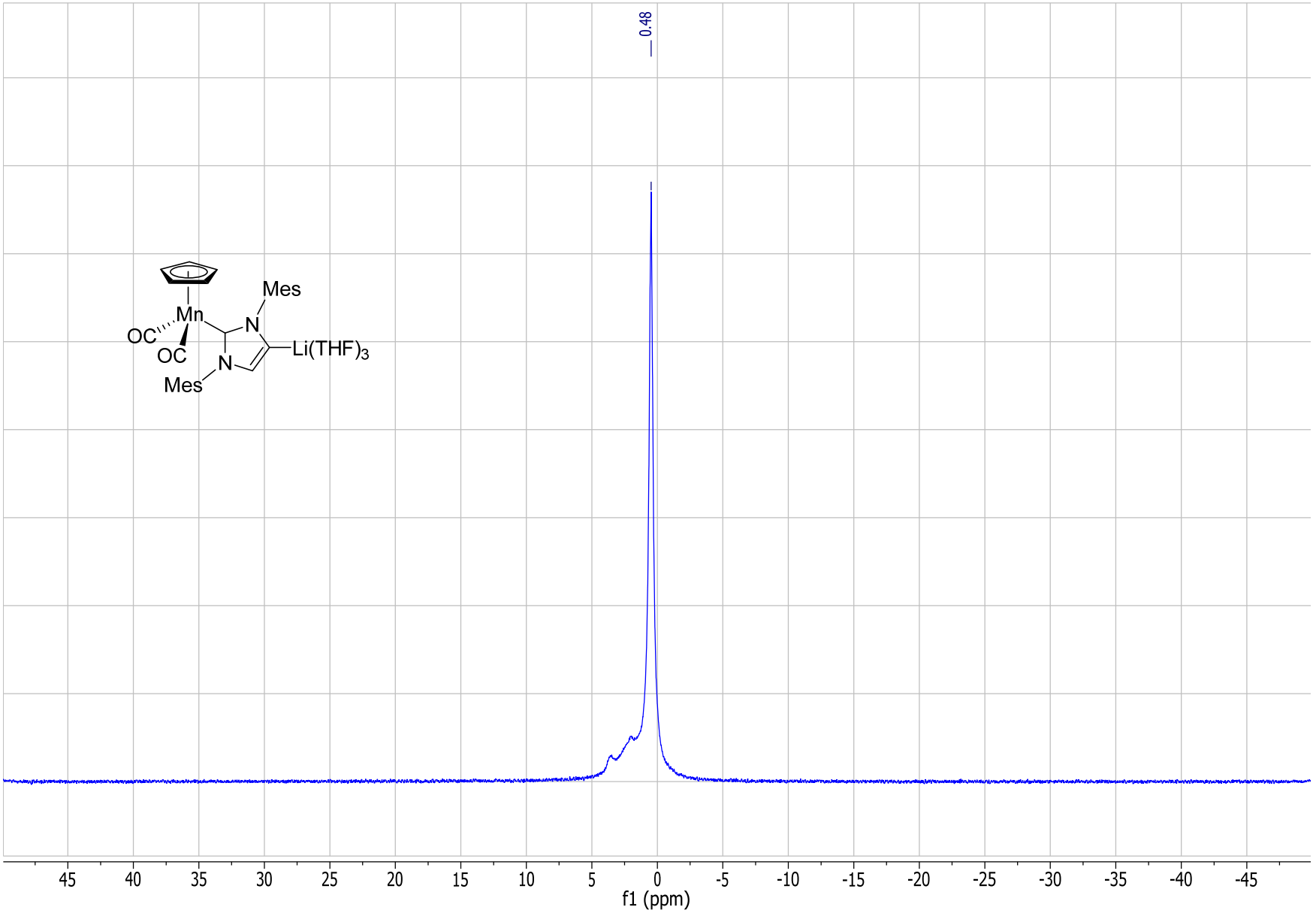

Figure 13S. ^{1}H NMR spectrum of complex **3** (400.1 MHz, $(CD_3)_2SO$, 25°C)

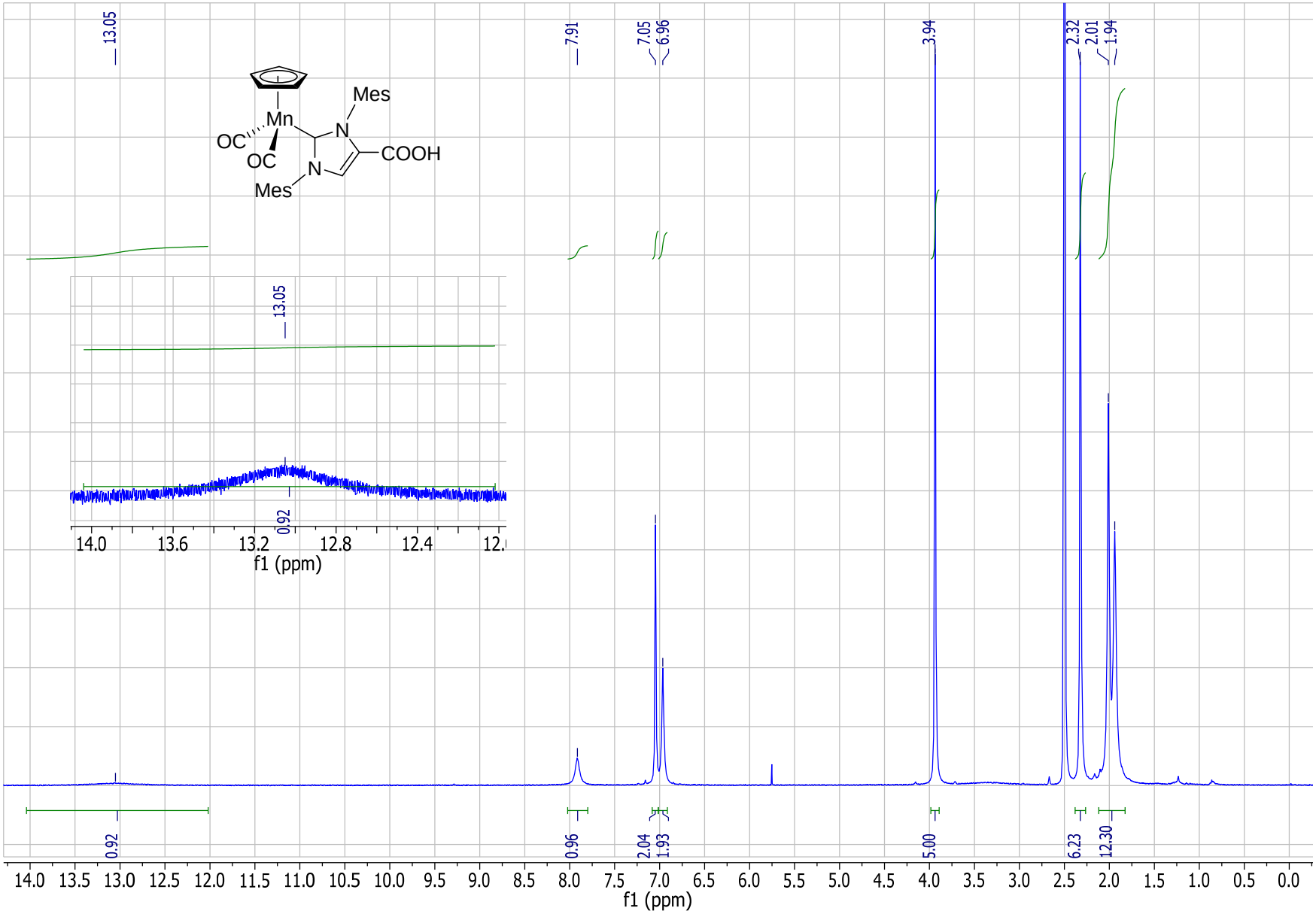

Figure 14S. $^{13}C\{^{1}H\}$ NMR spectrum of complex **3** (100.6 MHz, $(CD_3)_2SO$, 25°C)

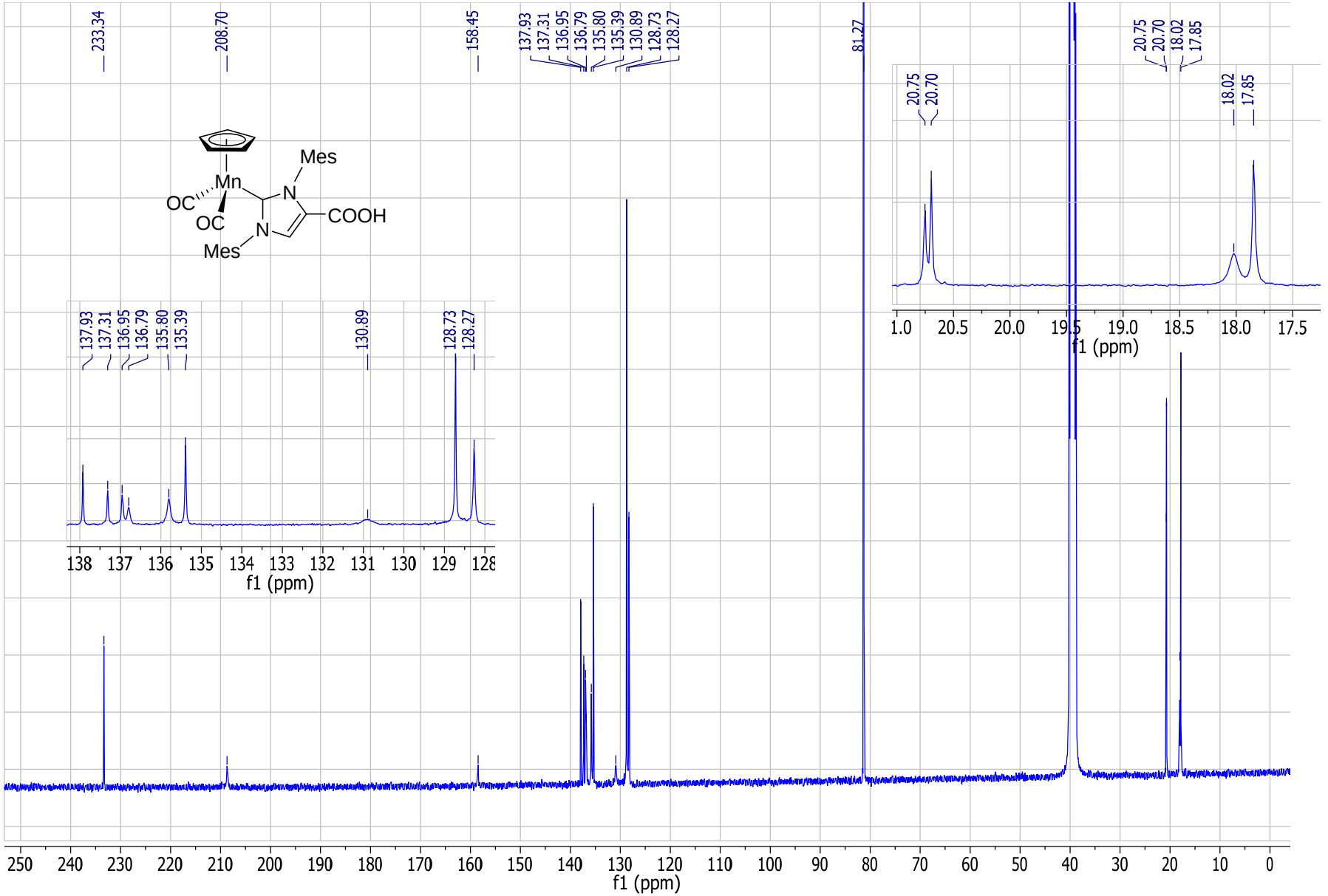

Figure 15S.[1]H NMR spectrum of complex **5** (400.1 MHz, CD_2Cl_2, 25°C)